Electronic Supplementary Material (ESI) for Chemical Communications

A new water-soluble pillar[5]arene: synthesis and application in the preparation of gold nanoparticles

Yong Yao,[a] Min Xue,[a] Xiaodong Chi,[a] Yingjie Ma,[a] Jiuming He,[b] Zeper Abliz,[b] and Feihe Huang[a,]*

[a] *Department of Chemistry, Zhejiang University, Hangzhou 310027, P. R. China, and Fax: +86-571- 8795-1895; Tel: +86-571-8795-3189; Email address: fhuang@zju.edu.cn.*

[b] *Institute of Materia Medica, Chinese Academy of Medical Sciences and Peking Union Medical College, Beijing 100050, P. R. China.*

Electronic Supplementary Information (23 pages)

1. Materials and methods

1,4-Bis(2-hydroxyethoxy)benzene, triphenylphosphine, carbon tetrabromide, boron trifluoride etherate and *N*-methylimidazole were reagent grade and used as received. Solvents were either employed as purchased or dried according to procedures described in the literatures. ^{1}H NMR spectra were collected on a Varian Unity INOVA-400 spectrometer (Bruker) with internal standard TMS. ^{13}C NMR spectra were recorded on a Varian Unity INOVA-400 spectrometry at 100 MHz. Mass spectra were obtained on a Bruker Esquire 3000 plus mass spectrometer (Bruker-Franzen Analytik GmbH Bremen, Germany) equipped with an ESI interface and an ion trap analyzer. HRMS were obtained on a Bruker 7-Tesla FT-ICRMS equipped with an electrospray source (Billerica, MA, USA). The melting points were collected on a SHPSIC WRS-2 automatic melting point apparatus.

*2. Syntheses of pillar[5]arene **1** and noncyclic monomeric analog **4***

Scheme S1. Synthetic route for compound **1**

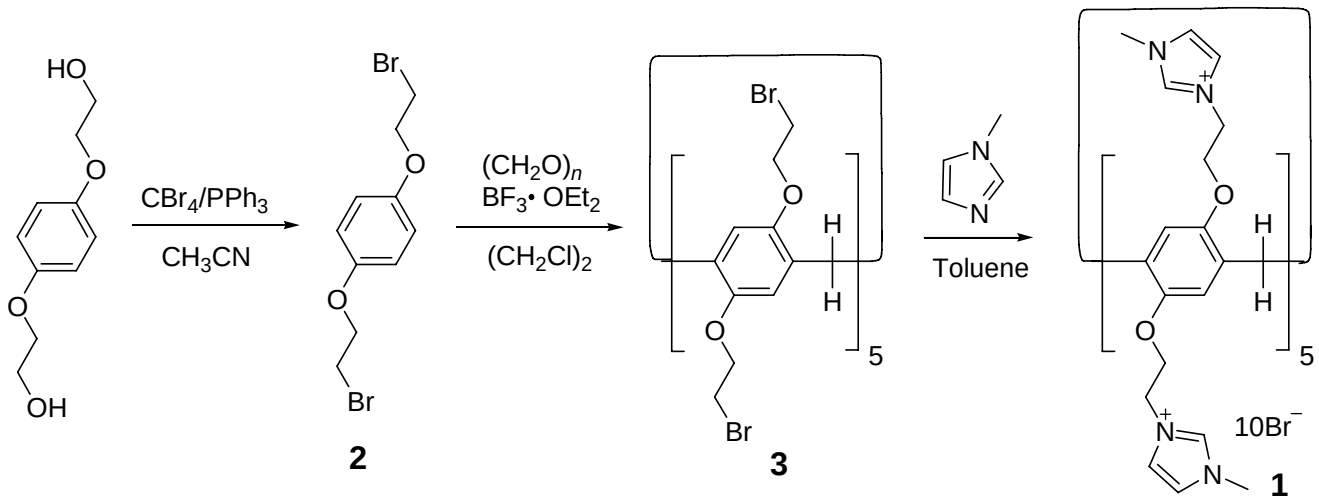

2.1. Synthesis of compound ***2***[S1,S2]

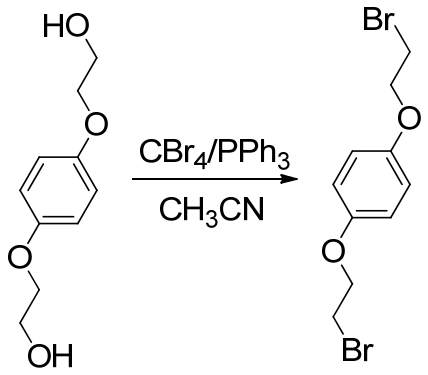

2

A solution of 1,4-bis(2-hydroxyethoxy)benzene (10.0 g, 50.4 mmol) and triphenylphosphine (31.5 g, 120 mmol) in dry acetonitrile (250 mL) was cooled with an ice bath. Under vigorous stirring, carbon tetrabromide (39.8 g, 120 mmol) was slowly added. The mixture was stirred at room temperature for 4 hours. Then cold water (200 mL) was added to the reaction mixture to give white precipitation. The precipitate was collected, washed with methanol/water (3:2, 3 × 100 mL), recrystallized from methanol, and dried under vacuum to afford **2** as white crystals (14.5 g, 94%). The ^{1}H NMR spectrum of **2** is shown in Figure S1. ^{1}H NMR (400 MHz, $CDCl_3$, rt) δ (ppm): 6.86 (s, 4H), 4.25 (t, J = 6.3 Hz, 4H), 3.62 (t, J = 6.8 Hz, 4H).

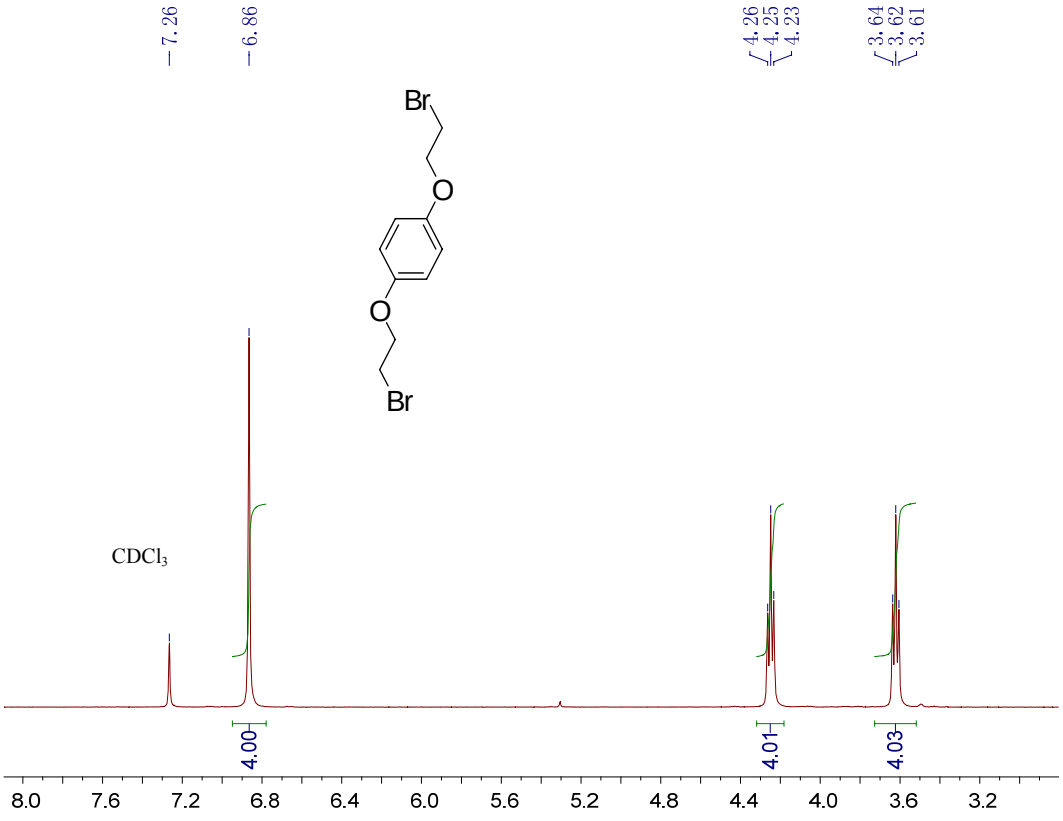

Fig. S1. ^{1}H NMR spectrum (400 Hz, $CDCl_3$, rt) of compound **2**.

2.2. Synthesis of compound ***3***[S1]

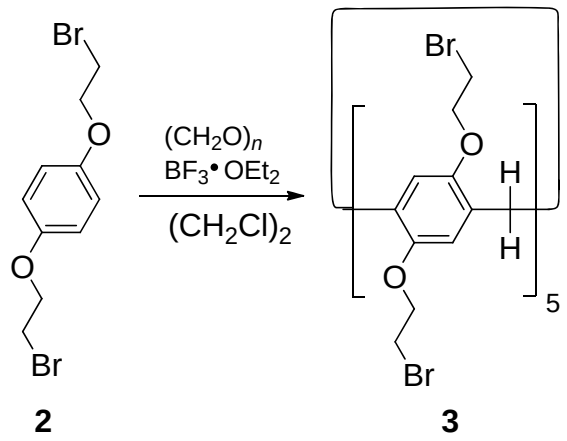

2 **3**

A solution of **2** (3.37 g, 11.5 mmol) and paraformaldehyde (0.349 g, 11.5 mmol) in 1,2-dichloroethane (50 mL) was cooled with ice bath. Boron trifluoride etherate (3.26 g, 23.0 mmol) was added to the solution and the mixture was stirred at room temperature for 1 hour. The reaction mixture was then washed with water (2 × 50 mL) and dried with Na_2SO_4. The solvent was evaporated to provide a crude product, which was purified by column chromatography (eluent: petroleum ether/ethyl acetate, 100:1) to afford a white solid (2.0 g, 52%). Mp: 93.2–95.8 ºC. The ^{1}H NMR spectrum of **3** is shown in Figure S2. ^{1}H NMR (400 MHz, $CDCl_3$, rt) δ (ppm): 6.93 (s, 10H), 4.24 (t, J = 5.7 Hz, 20H), 3.86 (s, 10H), 3.65 (t, J = 5.6 Hz, 20H).

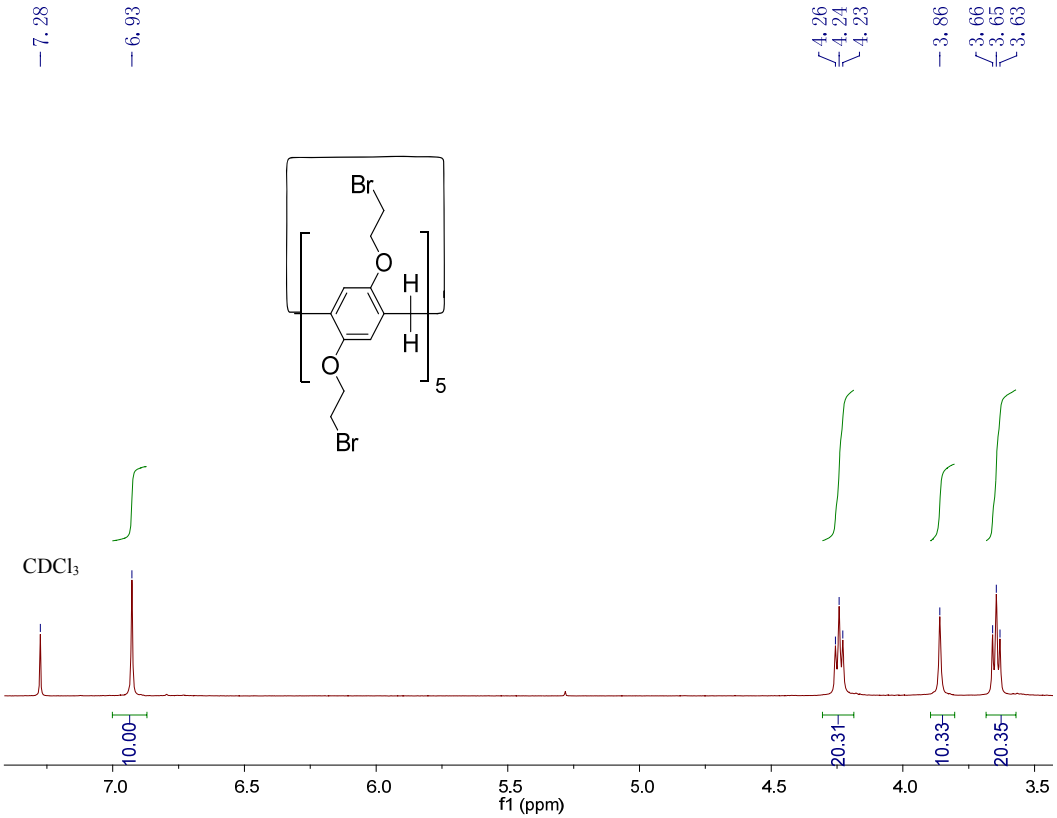

Fig. S2. ^{1}H NMR spectrum (400 MHz, $CDCl_3$, rt) of compound **3**.

2.3. Synthesis of compound ***1***

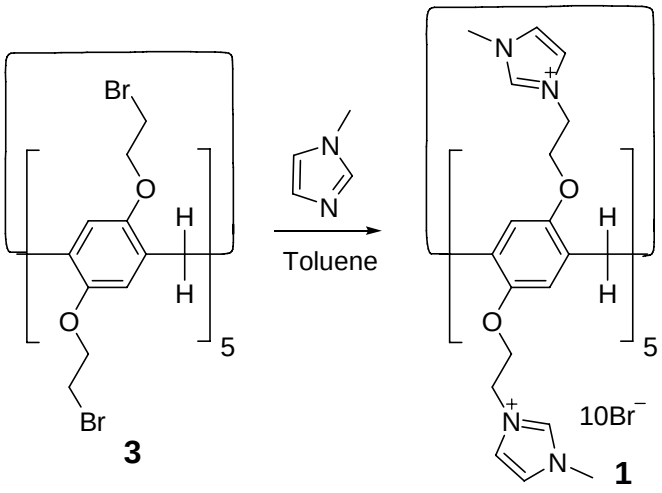

A mixture of **3** (1.68 g, 1.00 mmol) and *N*-methylimidazole (1.64 g, 20.0 mmol) in toluene (25 mL) was stirred in a 100 mL round-bottom flask at 120 ºC for 24 hours. After cooling, the solvent was removed and the residue was recrystallized from ethanol/diethyl ether (1:2) to give a white solid (2.1 g, 91%). Mp: 122.3–124.5 ºC. The ^{1}H NMR spectrum of **1** is shown in Figure S3. ^{1}H NMR (400 MHz, DMSO-d_6, rt) δ (ppm): 8.78 (s, 10H), 7.70 (s, 10H), 7.43 (s, 10H), 6.72 (s, 10H), 4.60 (s, 20H), 4.27 (s, 20H), 3.74 (s, 30H), 3.52 (s, 10H). The ^{13}C NMR spectrum of **1** is shown in Figure S4. ^{13}C NMR (100 MHz, DMSO-d_6, rt) δ (ppm): 149.02, 137.02, 128.41, 122.84, 118.19, 114.53, 66.69, 49.34, 40.01, 36.02, 28.84. HRESIMS is shown in Figure S5: *m/z* of $[M - 2Br]^{2+}$ $C_{95}H_{121}O_{10}N_{20}Br_8$ 1170.65; $[M - 3Br]^{3+}$ $C_{95}H_{121}O_{10}N_{20}Br_7$ 754.13; $[M - 4Br]^{4+}$ $C_{95}H_{121}O_{10}N_{20}Br_6$ 545.37; $[M - 5Br]^{5+}$ $C_{95}H_{121}O_{10}N_{20}Br_5$ 420.51; $[M - 6Br]^{6+}$ $C_{95}H_{121}O_{10}N_{20}Br_4$ 336.94; $[M - 7Br]^{7+}$ $C_{95}H_{121}O_{10}N_{20}Br_3$ 277.53.

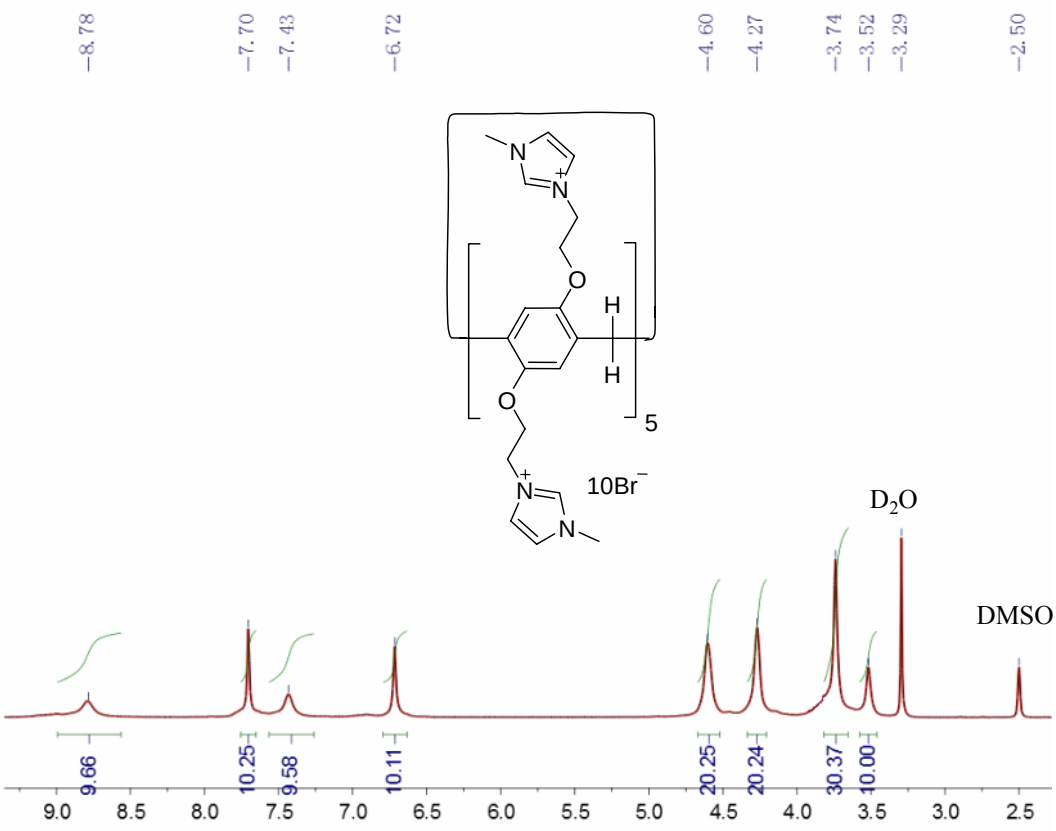

Figure S3. ^{1}H NMR spectrum (400MHz, DMSO-d_6, rt) of **1**.

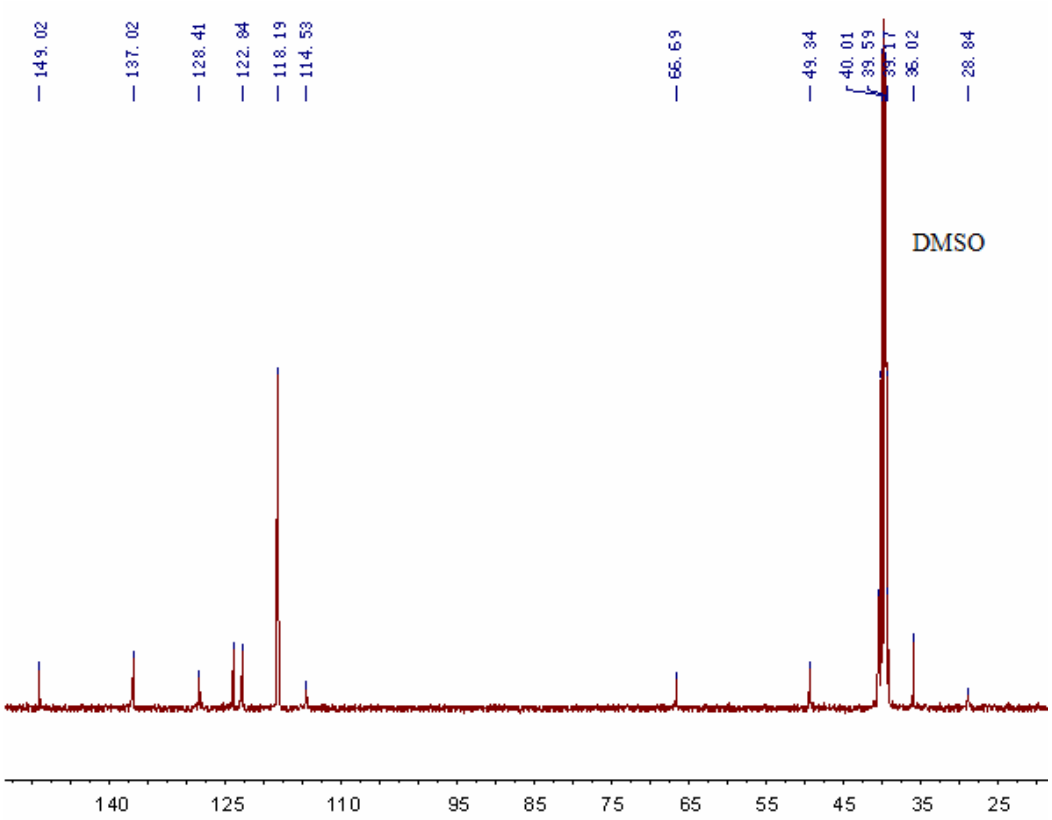

Fig. S4. ^{13}C NMR spectrum (100MHz, DMSO-d_6, rt) of **1**.

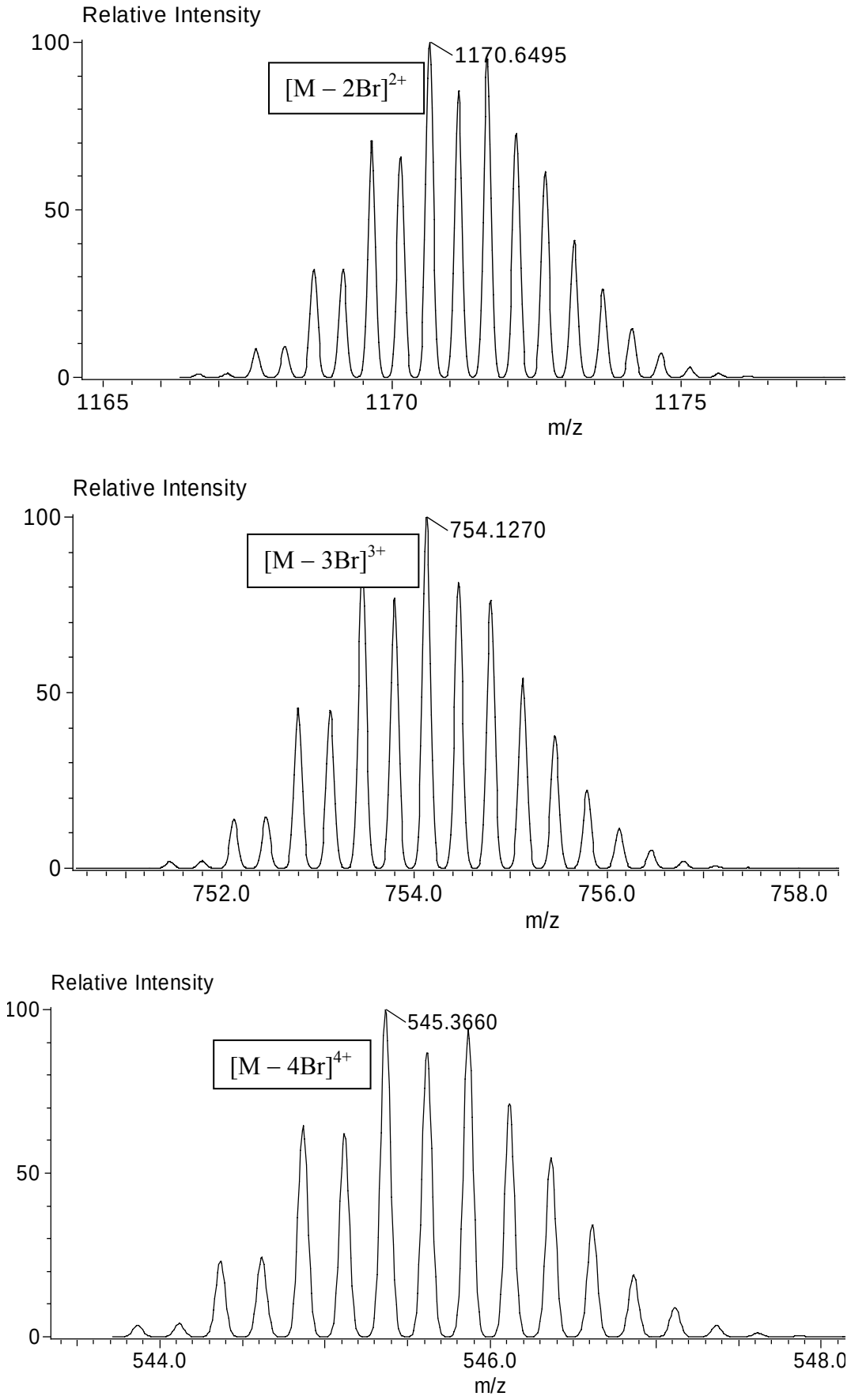
Relative Intensity
100
50
0
1170.6495
[M – 2Br]2+
1165
1170
1175
m/z
Relative Intensity
100
50
0
754.1270
[M – 3Br]3+
752.0
754.0
756.0
758.0
m/z
Relative Intensity
100
50
0
545.3660
[M – 4Br]4+
544.0
546.0
548.0
m/z

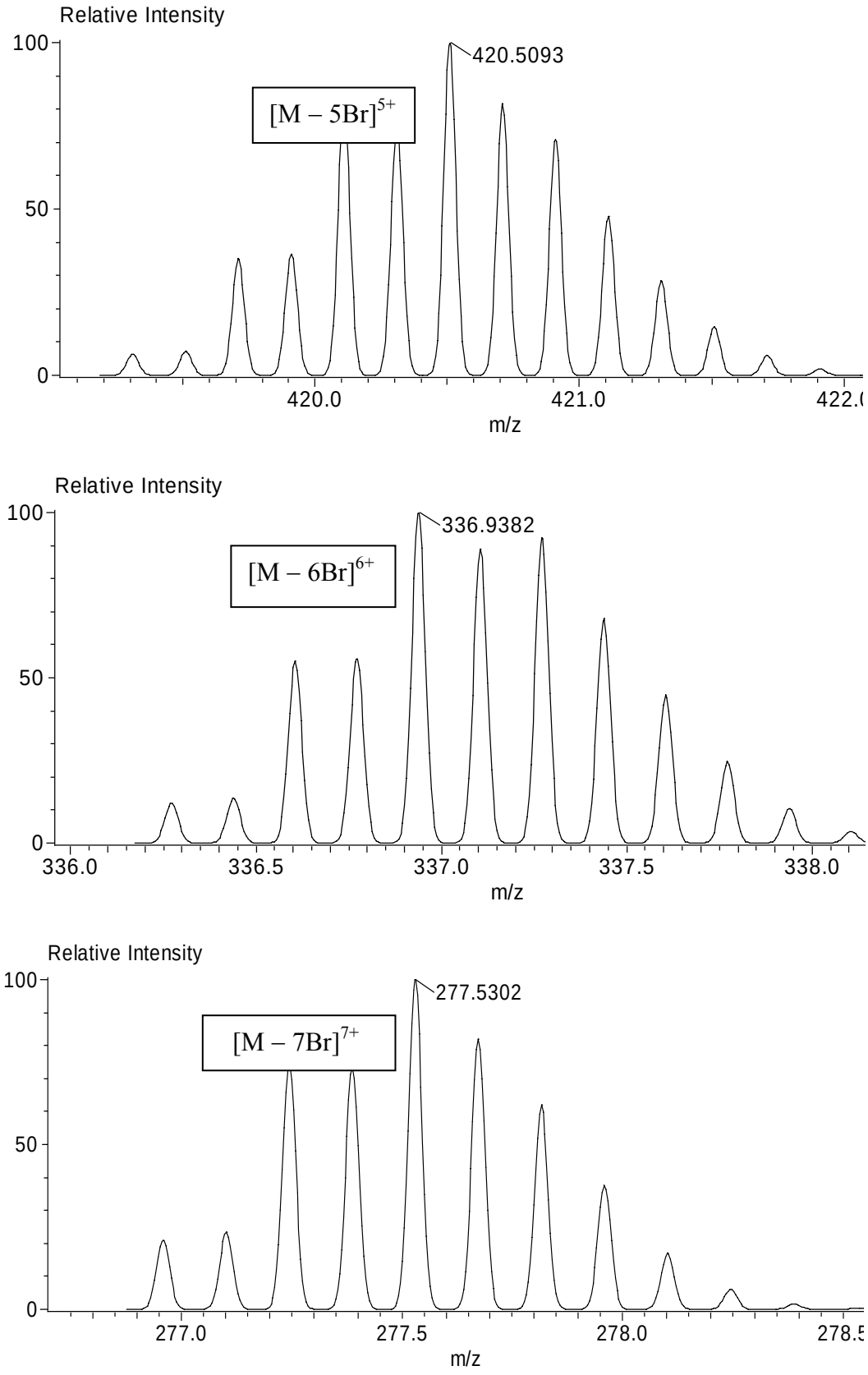

Fig. S5. High resolution electrospray ionization mass spectrum of **1**.

2.4 Synthesis of noncyclic monomeric analog ***4***

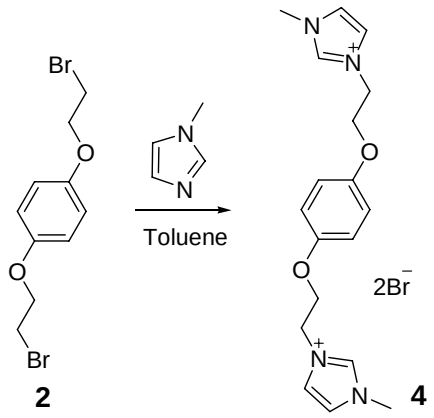

A mixture of **2** (1.68 g, 5.00 mmol) and *N*-methylimidazole (1.64 g, 20.0 mmol) in toluene (25 mL) was stirred in a 100 mL round-bottom flask at 120 ºC for 24 h. After cooling, the solvent was removed and the residue was recrystallized from ethanol/diethyl ether (1:2) to give a white solid (2.3 g, 96%). Mp: 98.7–99.4 ºC. The ^{1}H NMR spectrum of **4** is shown in Figure S6. ^{1}H NMR (400 MHz, D_2O, rt) δ (ppm): 8.74 (s, 2H), 7.50 (s, 2H), 7.37 (s, 2H), 6.88 (s, 4H), 4.51 (t, J = 4.0 Hz, 4H), 4.33 (t, J = 4.0 Hz, 4H), 3.82 (s, 6H). The ^{13}C NMR spectrum of **4** is shown in Figure S7. ^{13}C NMR (100 MHz, DMSO-d_6, rt) δ (ppm): 152.11, 136.33, 123.38, 122.49, 115.97, 66.60, 48.84, 35.63. LRESIMS is shown in Figure S8: *m/z* 640.0 $[M - 2Br]^{2+}$. HRESIMS is shown in Figure S9: *m/z* calcd for $[M - Br]^{+}$ $C_{18}N_4BrO_2H_{24}$, 407.1077; found 407.1077.

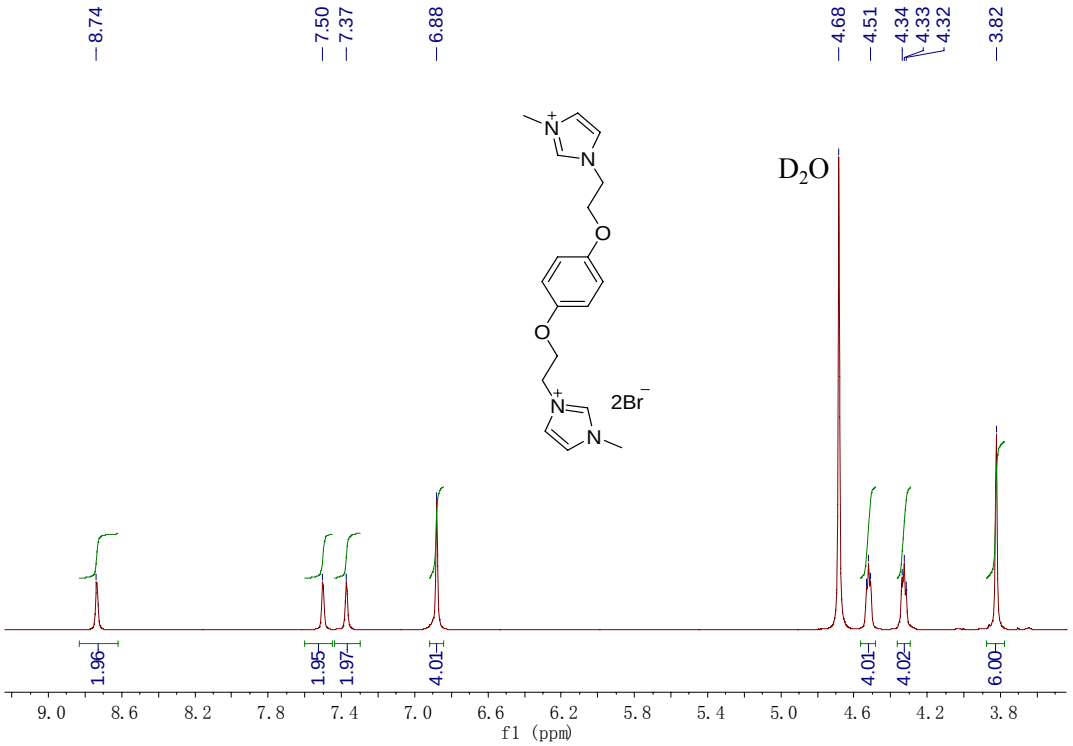

Fig. S6. ^{1}H NMR spectrum (400MHz, D_2O, rt) of **4**.

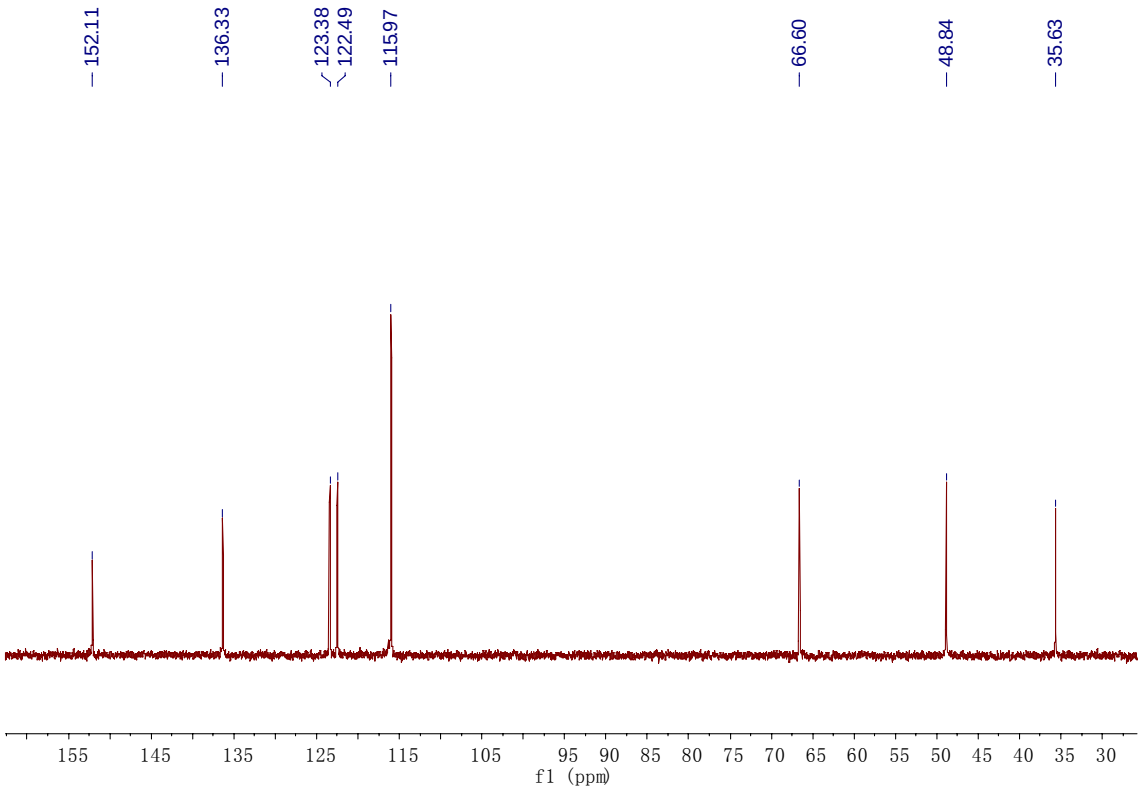

Fig. S7. ^{13}C NMR spectrum (100MHz, D_2O, rt) of **4**.

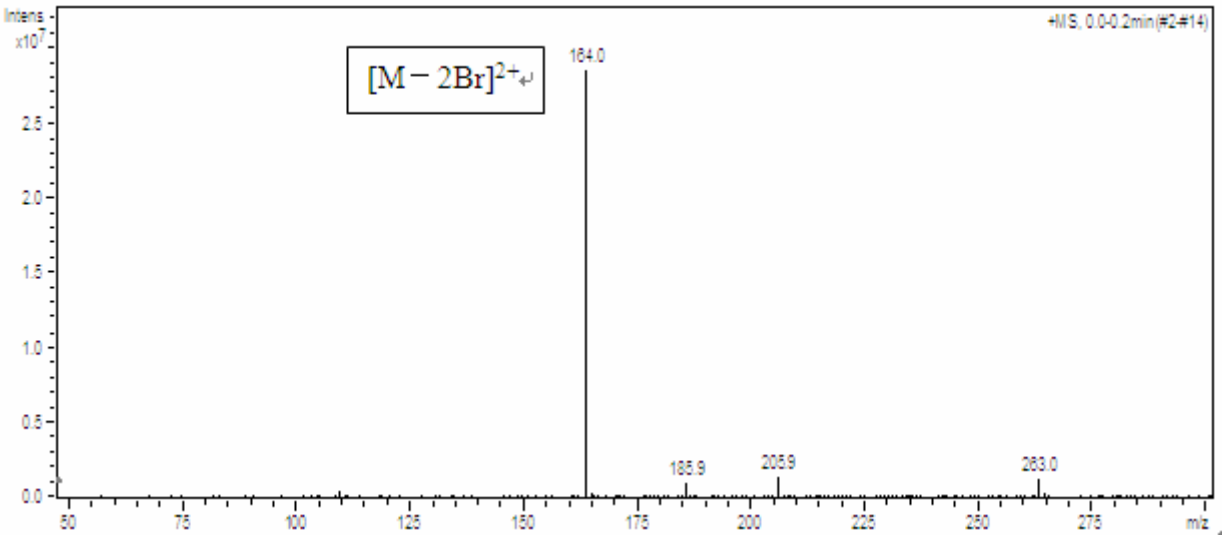

Fig. S8. Electrospray ionization spectrum of **4**. Assignment of the main peak: *m*/*z* 164.0 $[M - 2Br]^{2+}$.

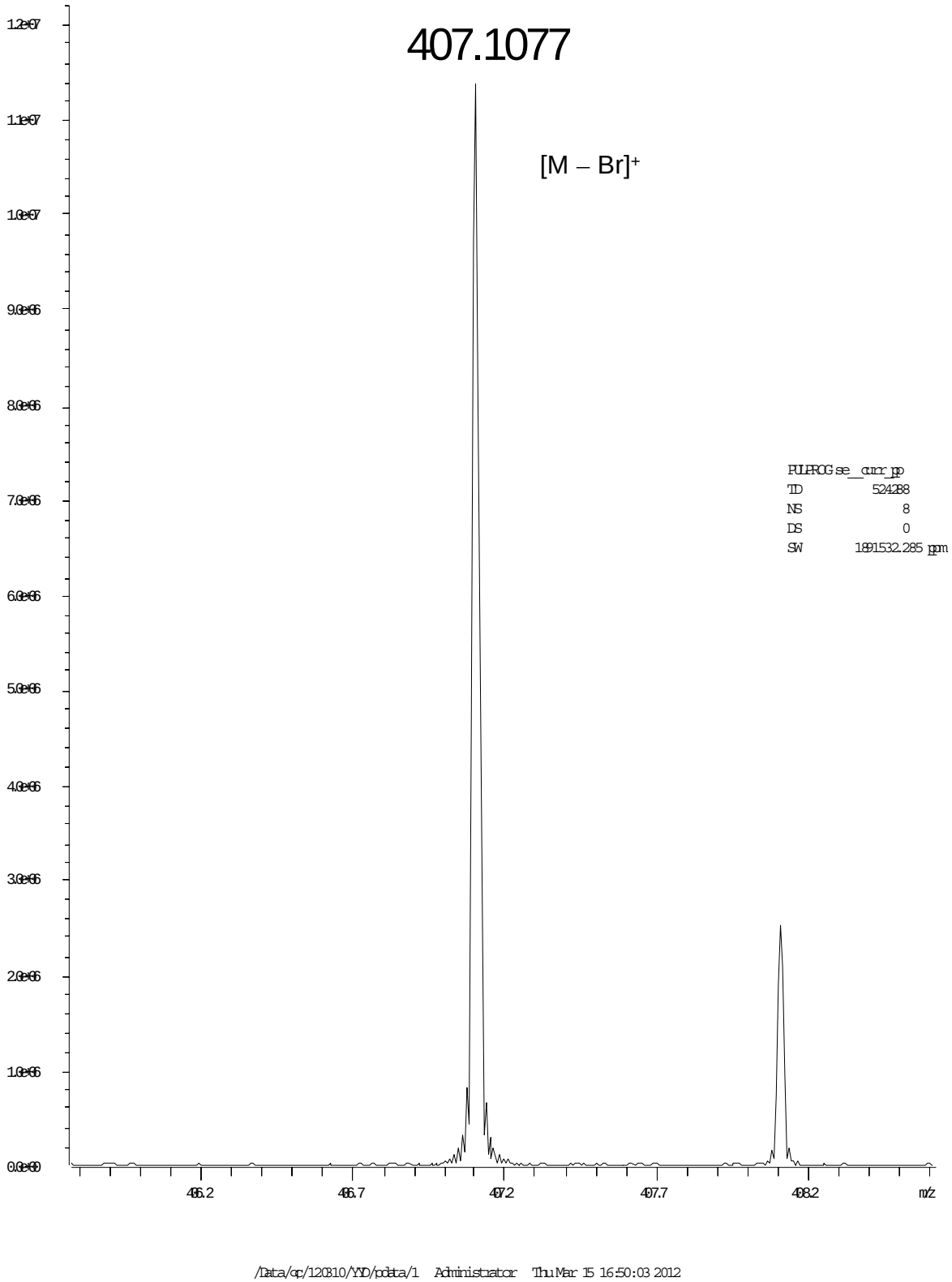

Fig. S9. High resolution electrospray ionization mass spectrum of **4**.

3. Synthesis and characterization of pillar[5]arene-stabilized gold nanoparticles

3.1. Synthesis of gold nanoparticles

The GNPs were synthesized by the reduction of $AuCl_4^-$ ions in the aqueous dispersions of **1**. In a typical experiment, an aqueous solution of $HAuCl_4$ (0.10 mL, 9.7 mM) was added to an aqueous solution of **1** (2.7 mL, 10^{-1} mM). Then aqueous sodium borohydride (0.20 mL, 0.0125 g/mL) was injected into the above solution under vigorous stirring. The solution became wine red, indicating that pillar[5]arene-stabilized gold nanoparticles were immediately obtained.

3.2 Characterization of gold nanoparticles

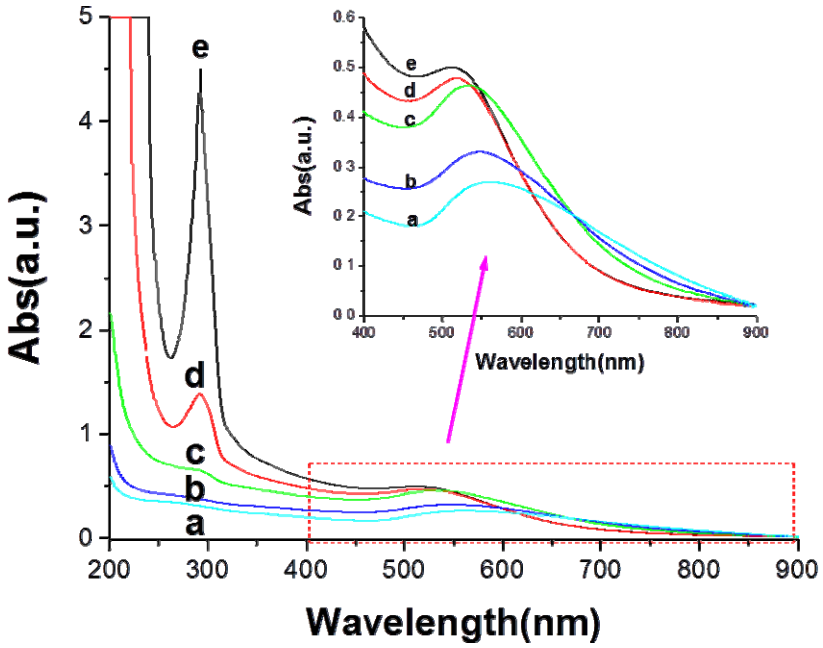

Fig. S10. UV/Vis spectra of gold nanoparticles stabilized by pillar[5]arene **1** at different concentrations: a, 2 μM; b, 4 μM; c, 10 μM; d, 50 μM; e, 200 μM.

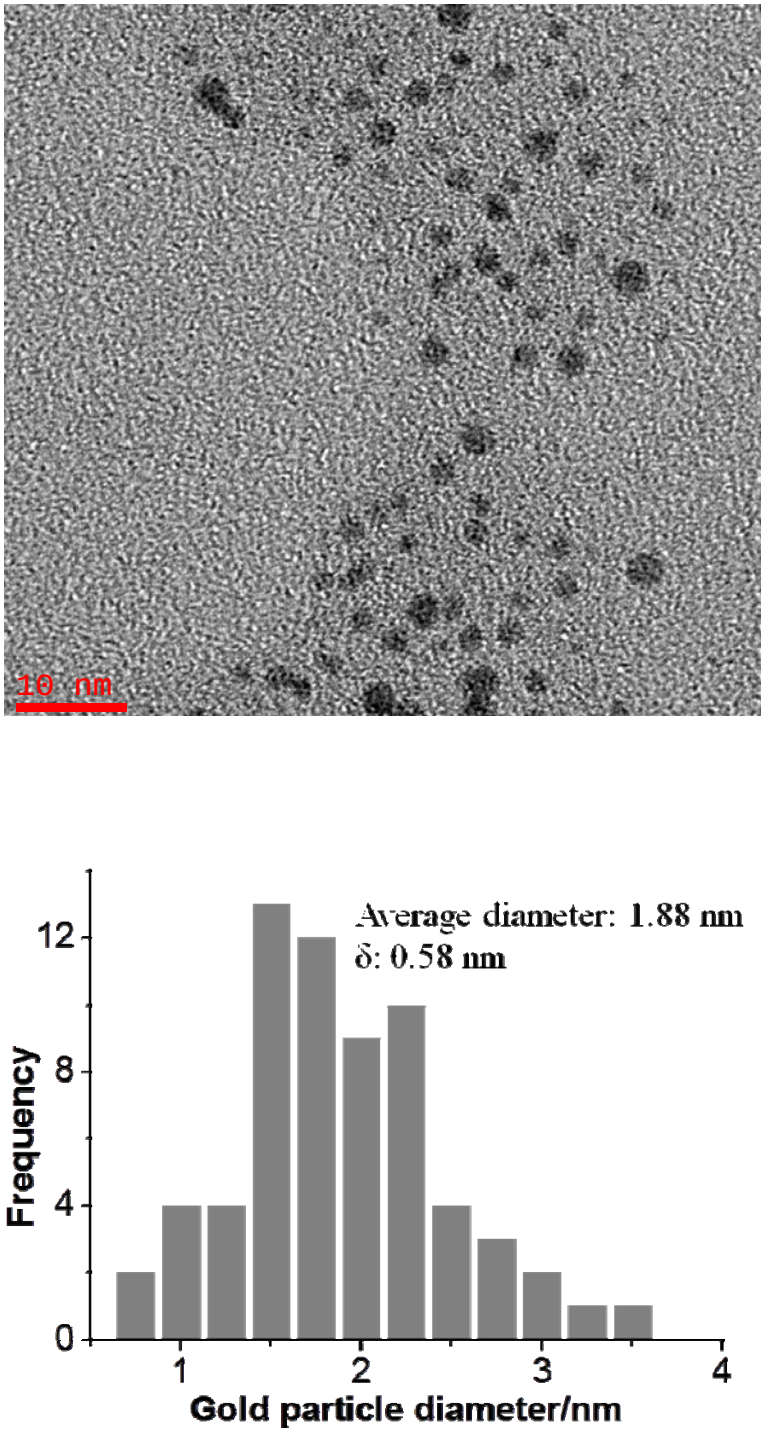

Fig. S11. TEM image and size histogram of gold nanoparticles stabilized by **1** at a concentration of 200 μM.

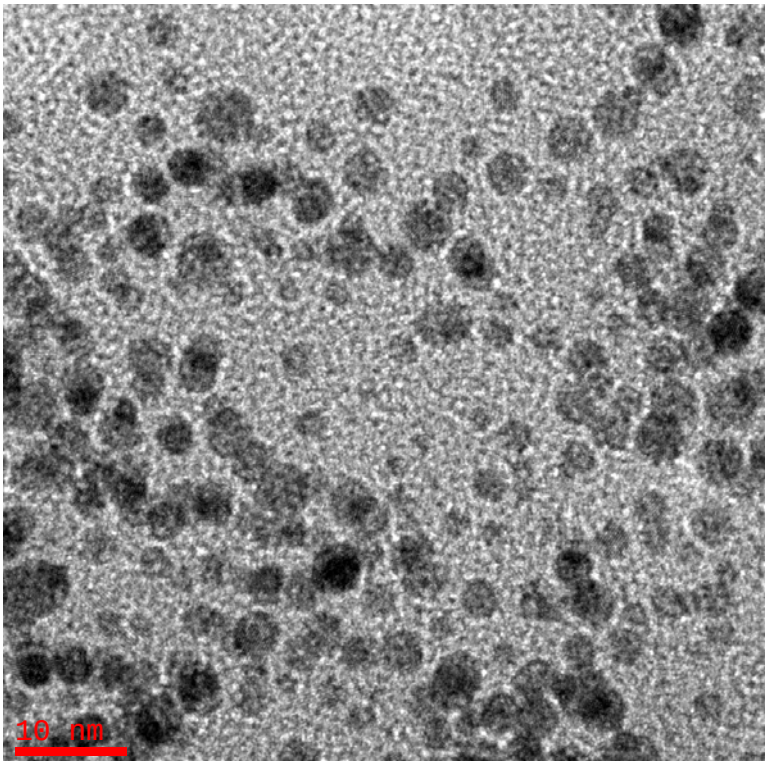

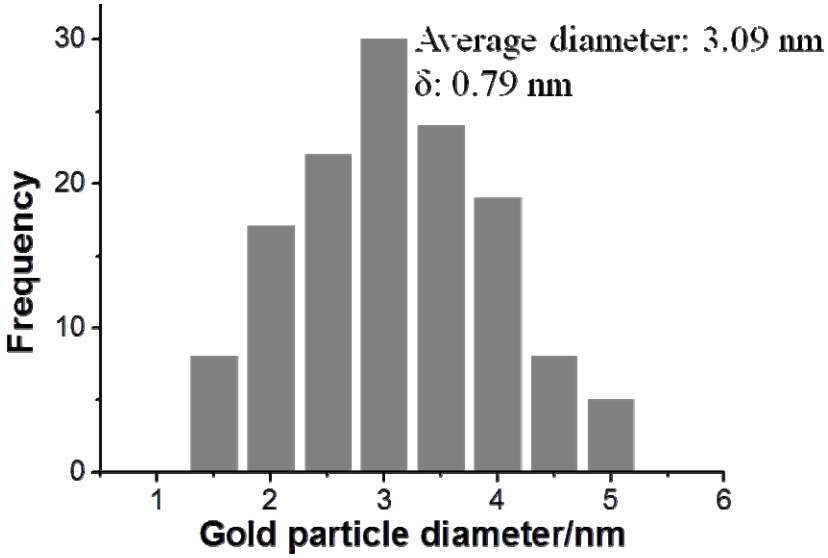

Fig. S12. TEM image and size histogram of gold nanoparticles stabilized by **1** at a concentration of 50 μM.

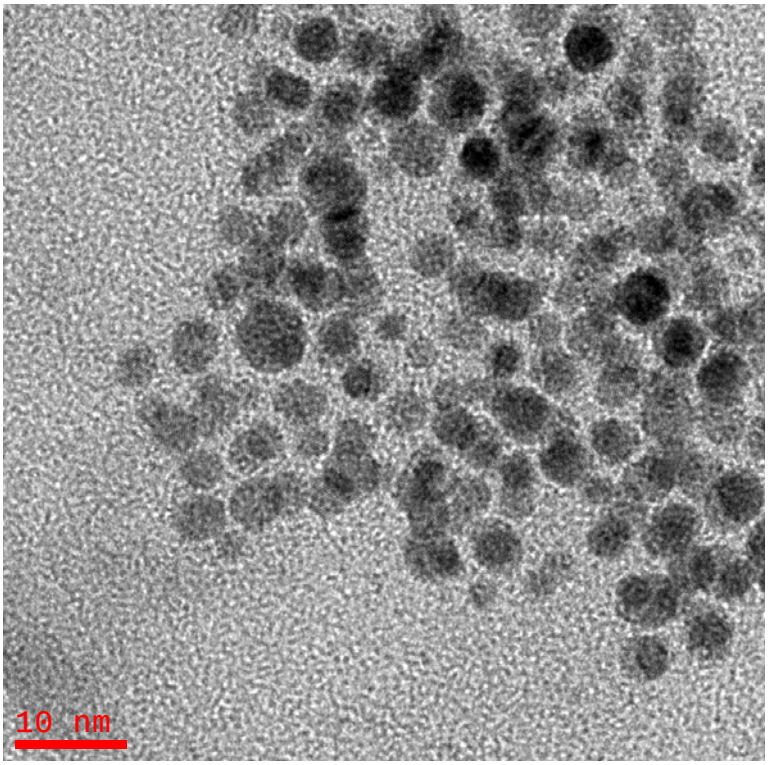

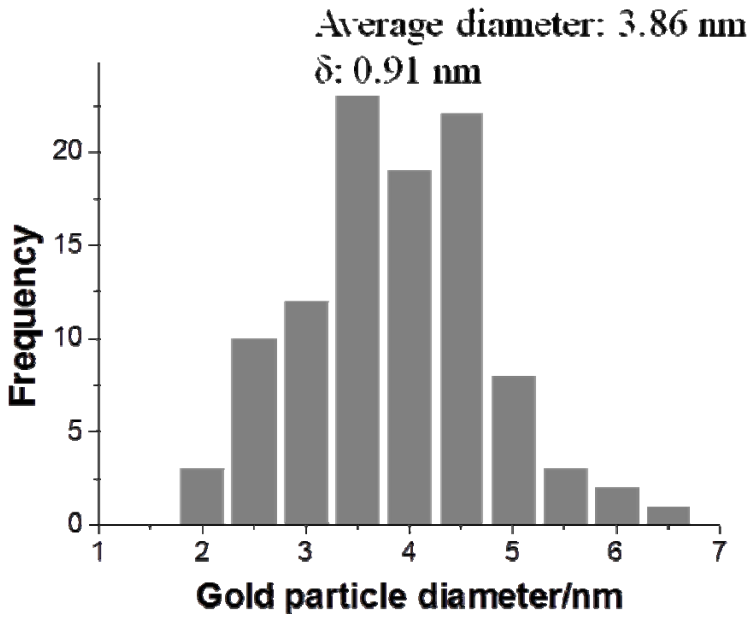

Fig. S13. TEM image and size histogram of gold nanoparticles stabilized by **1** at a concentration of 10 μM.

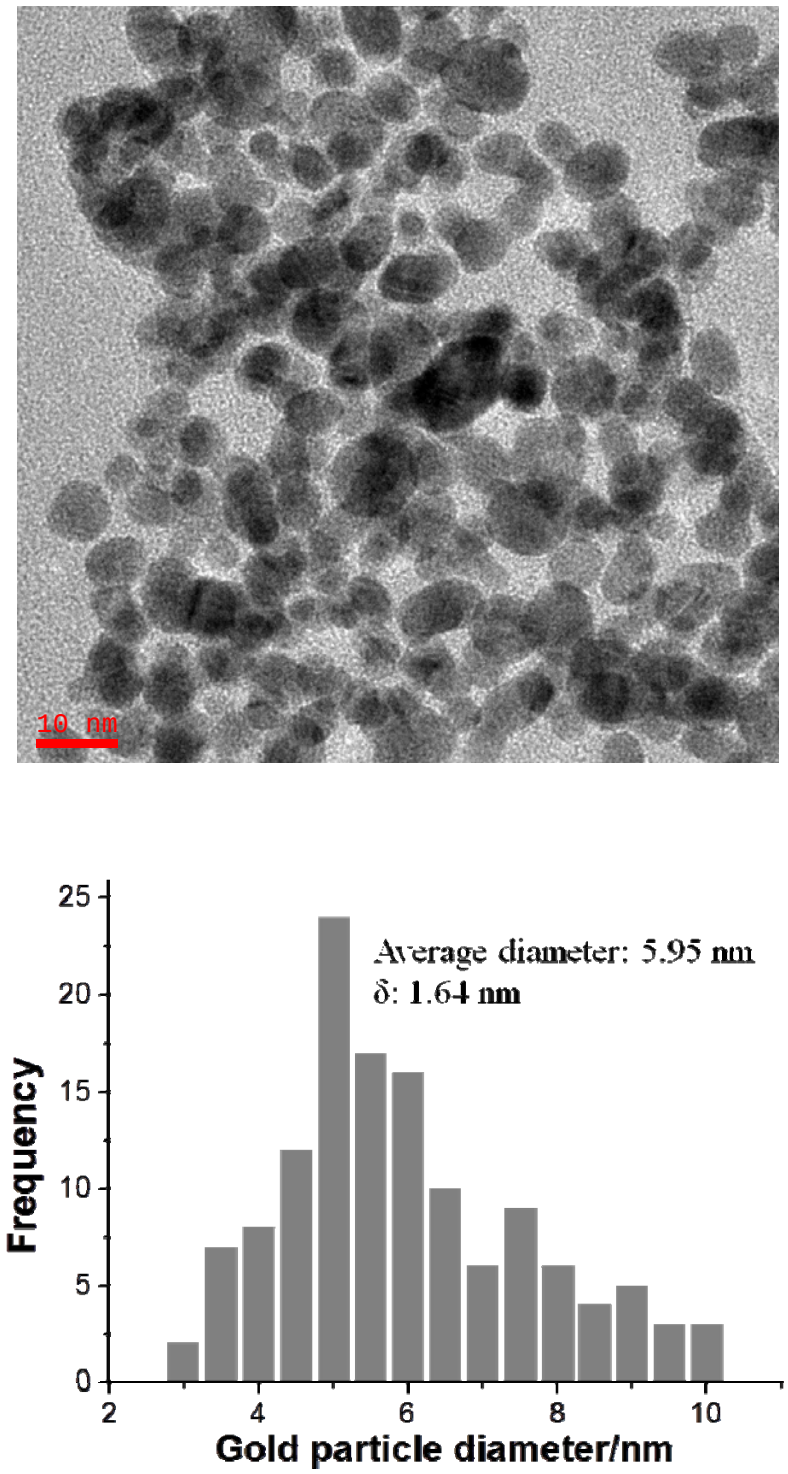

Fig. S14. TEM image and size histogram of gold nanoparticles stabilized by **1** at a concentration of 2 μM.

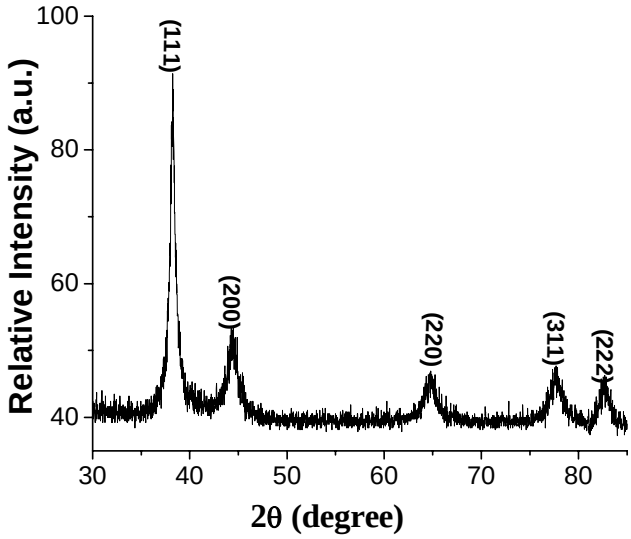

Fig. S15. XRD pattern of gold nanoparticles.

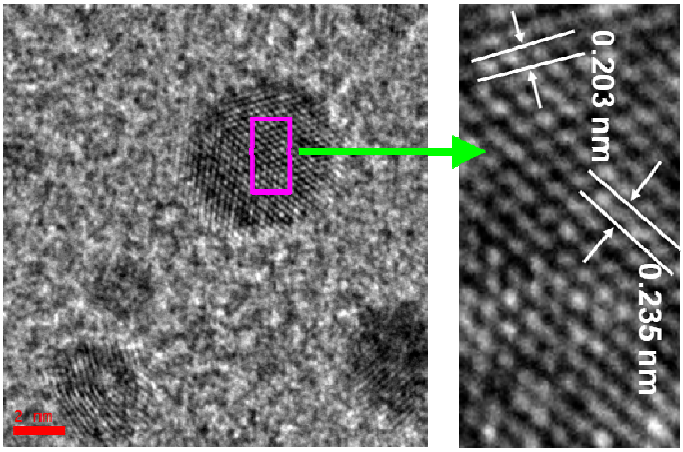

Fig. S16. High-resolution TEM image of gold nanoparticles stabilized by pillar[5]arene **1** with a concentration of 200 μM (scale bar: 2 nm).

4. Catalytic reduction of 4-nitroaniline

The catalytic reduction of 4-nitroaniline was studied as follows. To a standard quartz cell with a 1-cm path length and about 4 mL volume, 3 mL of 0.20 mM 4-nitroaniline and 0.03 g of $NaBH_4$ (much more excess) were added. Then the addition of 0.01 mL of 2.0×10^{-3} mM gold nanoparticles to the mixture caused the decrease in the intensity of the absorption of 4-nitroaniline. The absorption spectra were recorded every 2 minutes in a scanning range of 200–700 at room temperature. The control experiment was also carried out using a mixture of $NaBH_4$ and 4-nitroaniline.

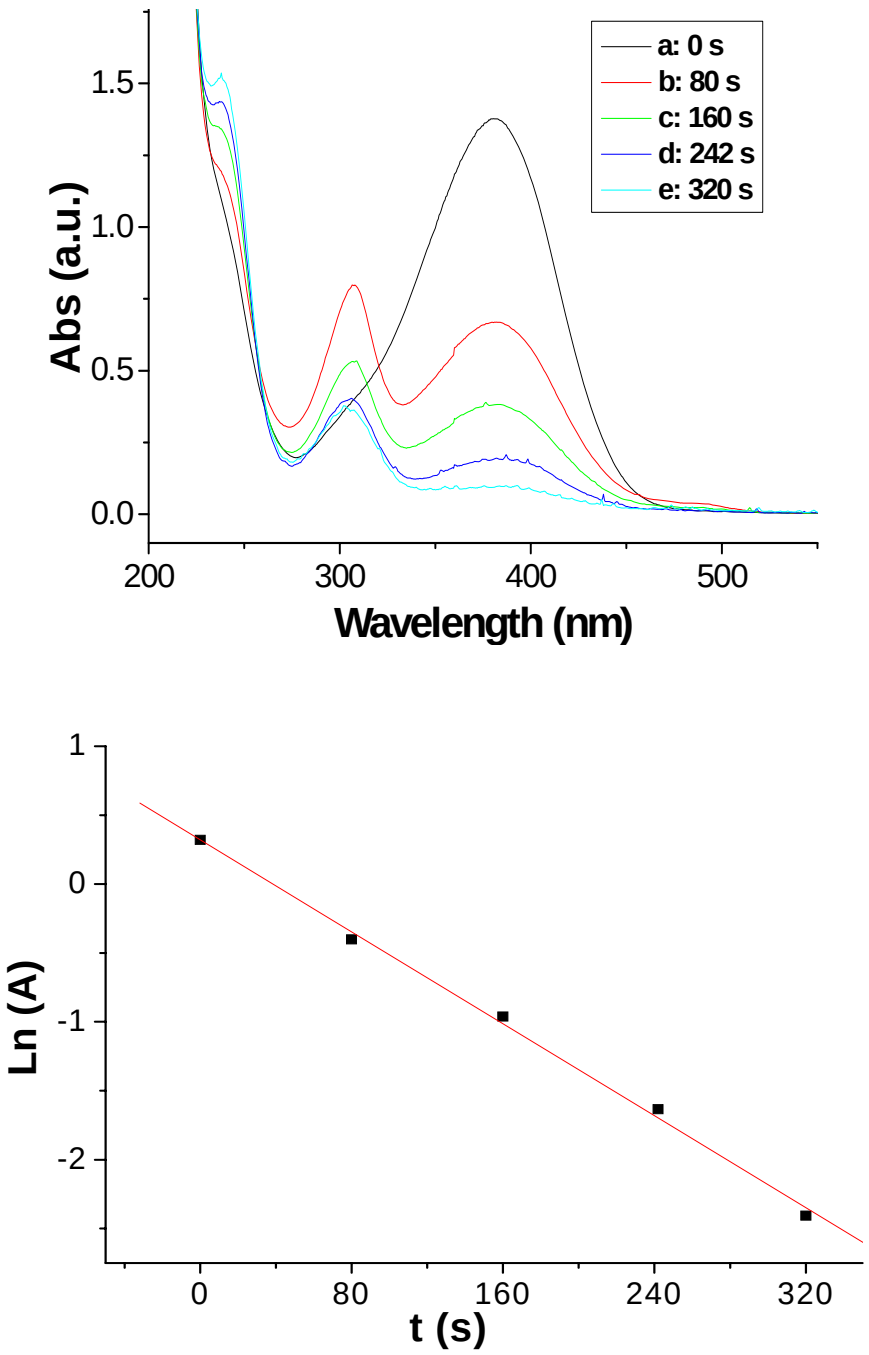

Fig. S17. The successive UV/Vis absorption of the reduction of 4-nitroaniline and plot of ln(A) against time by excess $NaBH_4$ in the presence of pillar[5]arene-stabilized gold nanoparticles with an average size of 1.88 ± 0.58 nm.

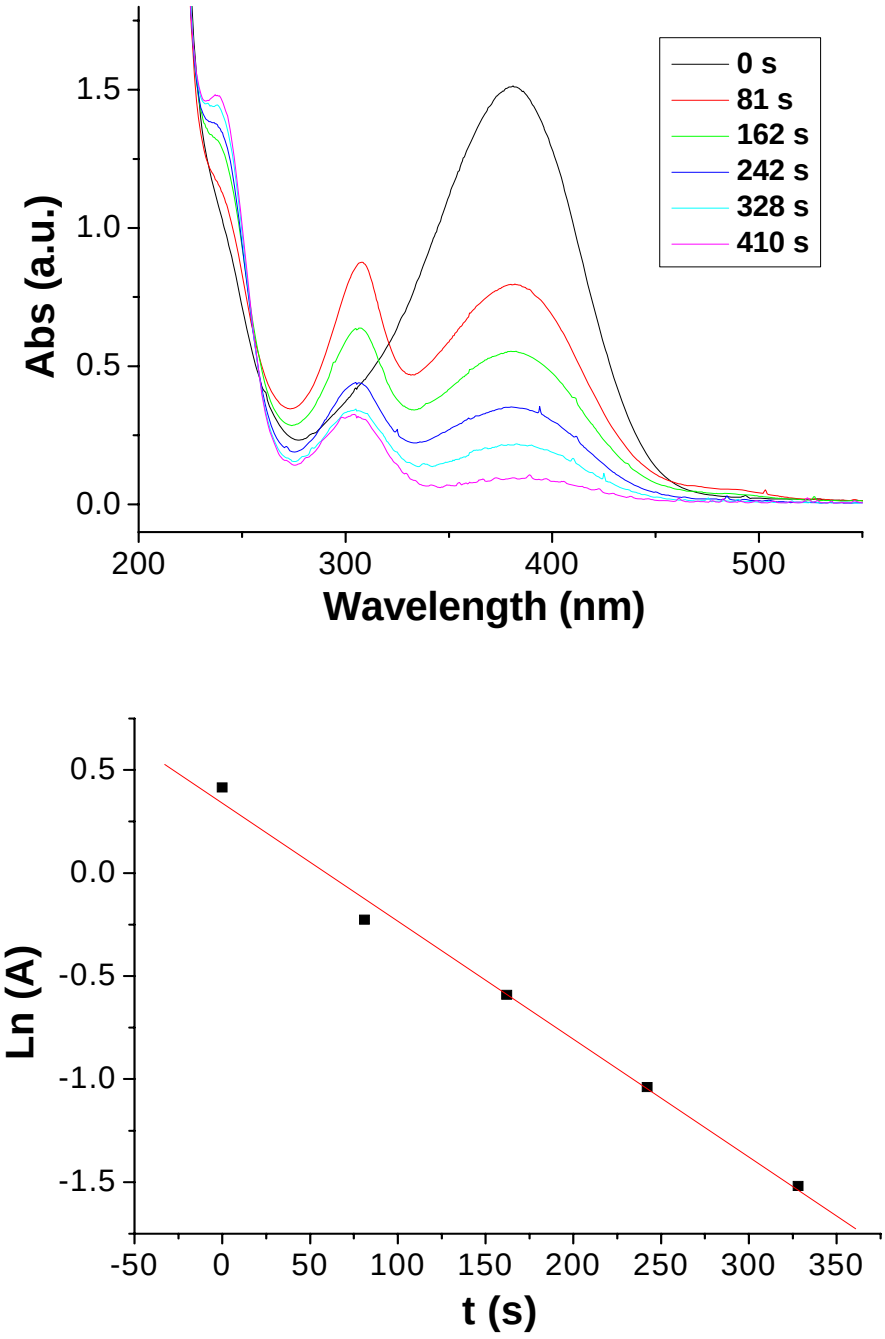

Fig. S18. The successive UV/Vis absorption of the reduction of 4-nitroaniline and plot of ln(A) against time by excess $NaBH_4$ in the presence of pillar[5]arene-stabilized gold nanoparticles with an average size of 3.09 ± 0.79 nm.

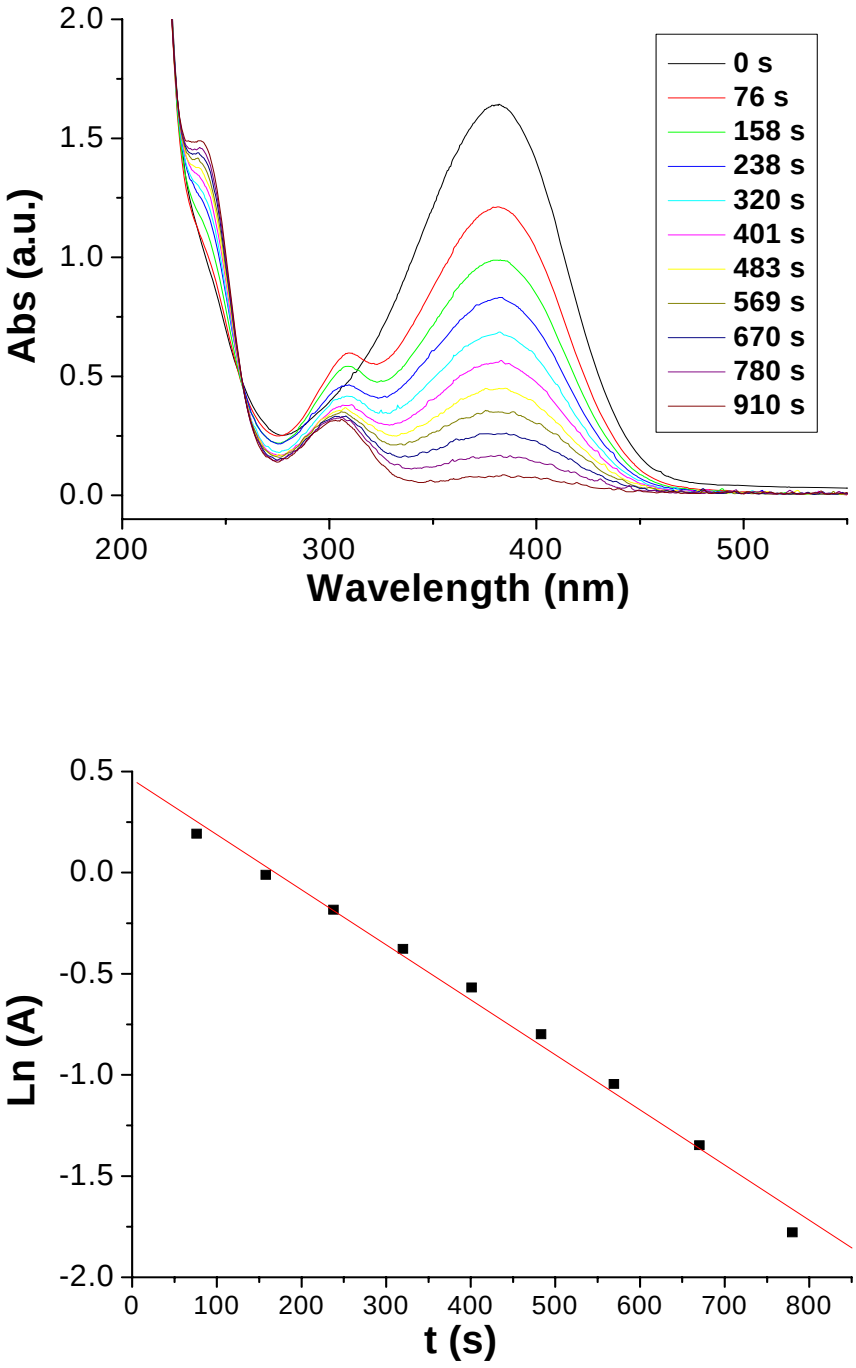

Fig. S19. The successive UV/Vis absorption of the reduction of 4-nitroaniline and plot of ln(A) against time by excess $NaBH_4$ in the presence of pillar[5]arene-stabilized gold nanoparticles with an average size of 3.86 ± 0.91 nm.

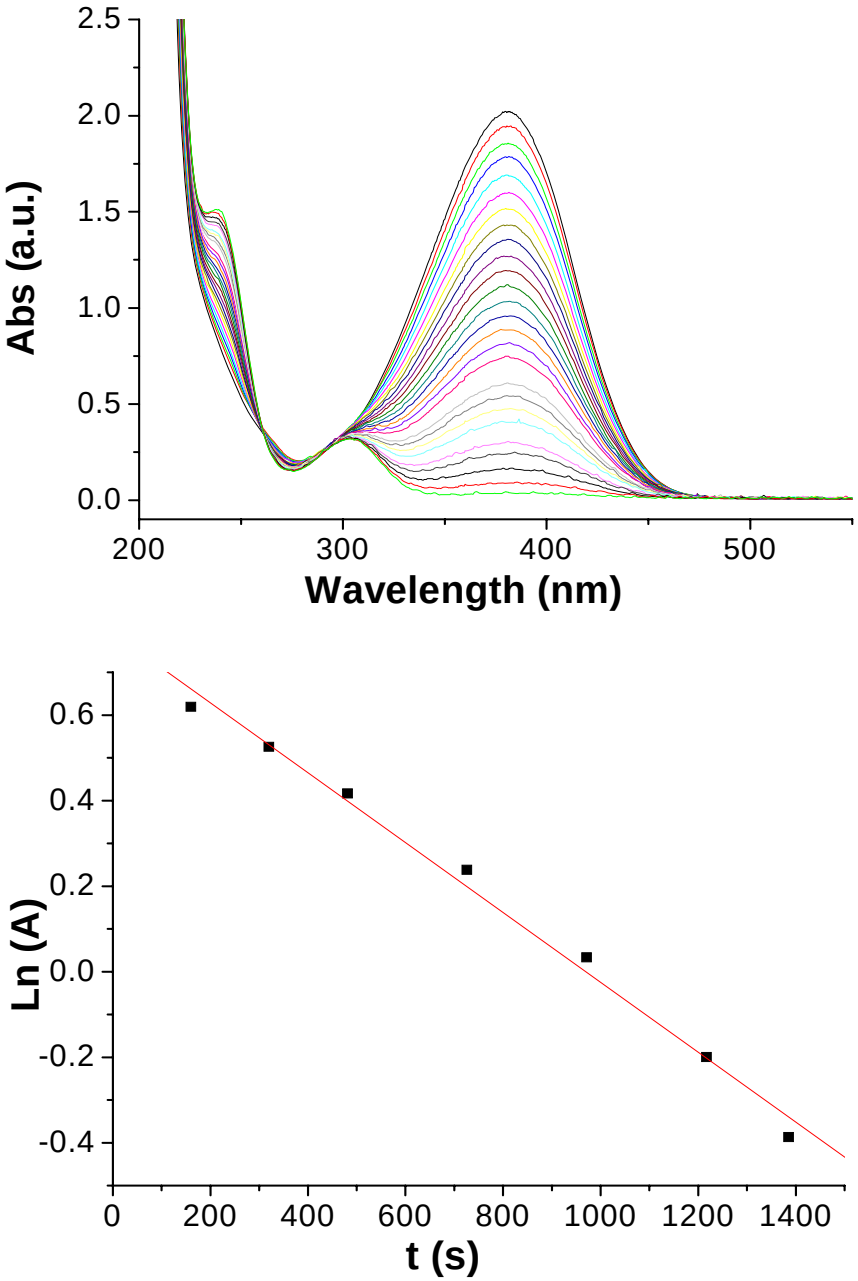

Fig. S20. The successive UV/Vis absorption of the reduction of 4-nitroaniline and plot of ln(A) against time by excess $NaBH_4$ in the presence of pillar[5]arene-stabilized gold nanoparticles with an average size of 5.95 ± 1.64 nm.

Tab. S1. Au nanoparticles as catalysts for the borohydride reduction of nitro-compounds

Catalyst	Mole ratio (HAuCl/nitro-compound)	Nitro-compound	Reaction rate constant	References
Au nanoparticles	0.2%	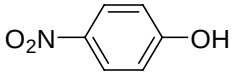	$7.36 \times 10^{-3}\ S^{-1}$	S3
Au@SiO_2 core-shell particles	50%	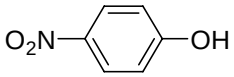	$4.6 \times 10^{-4}\ S^{-1}$	S4
Road-Shaped Gold Nanorattles	0.5%	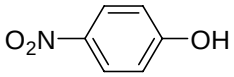	$< 10^{-2}\ S^{-1}$	S5
Au Nanocrystals	18%	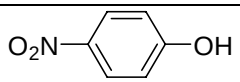	$6.54 \times 10^{-3}\ S^{-1}$	S6
Au nanoparticles	1%	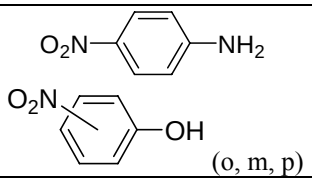 (o, m, p)	$< 5 \times 10^{-3}\ S^{-1}$	S7
This work	0.08%	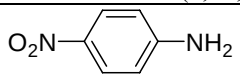	$8.34 \times 10^{-3}\ S^{-1}$	

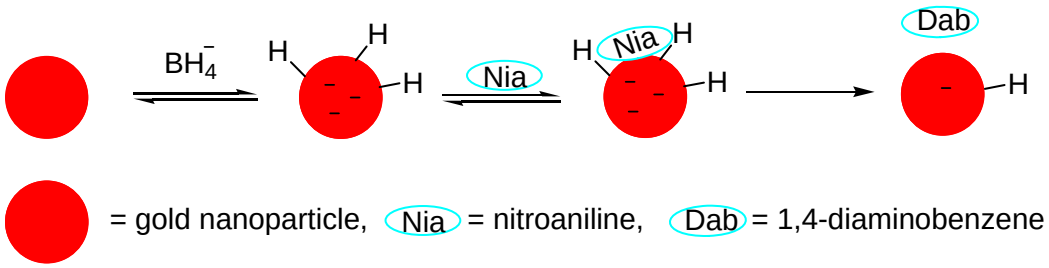

Fig. S21. Mechanistic model of the reduction of 4-nitroaniline.

5. References:

S1. Y. Ma, X. Ji , F. Xiang, X. Chi, C. Han, J. He, Z. Abliz, W. Chen and F. Huang, *Chem. Commun.,* 2011, **47**, 12340–12342.

S2. M. R. Pinto, B. M. Kristal and K. S. Schanze, *Langmuir*, 2003, **19**, 6523–6533.

S3. Y. Gao, X. Ding, Z. Zheng, X. Cheng and Y. Peng, *Chem. Commun.*, 2007, 3720–3722.

S4. B. J. Lee, J. C. Park and H. Song, *Adv. Mater*., 2008, **20**, 1523–1528.

S5. Y. Khalavka, J. Becker and C. Sonnichsen, *J. Am. Chem. Soc.*, 2009, **131**, 1871–1875.

S6. J. Liu, G. Qin, P. Raveendran and Y. Ikushima, *Chem. Eur. J.*, 2006, **12**, 2131–2138.

S7. Y. Yao, Y. Sun, Y. Han and C. Yan, *Chin. J. Chem.*, 2010, **28**, 705–712.